ELSEVIER

Tectonophysics 307 (1999) 407–419

TECTONOPHYSICS

www.elsevier.com/locate/tecto

Postglacial crustal doming, stresses and fracture formation with application to Norway

Agust Gudmundsson *

Geological Institute, University of Bergen, Allegt. 41, N-5007 Bergen, Norway

Received 2 March 1998; accepted 25 February 1999

Abstract

Postglacial doming of Fennoscandia is estimated to have reached a maximum uplift value of 850 m. Vertical uplift of this magnitude generates stresses that affect the tectonic activity in the domed area. Using a simple model of a circular, elastic plate subject to deflection, it is shown that the maximum tensile stresses generated by this uplift occur in the centre of the dome, and at the surface reach a numerical value of nearly 30 MPa. This tensile stress is an order of magnitude greater than the typical in-situ tensile strength of the uppermost part of the crust, so that tension fractures are easily generated by this stress. Tension fractures can, under certain conditions, reach crustal depths of several hundred metres, but if they propagate to greater depths they change into normal faults. The tensile stresses at the surface decrease in magnitude with distance from the centre of the dome and become compressive in the marginal parts of the uplifted crustal plate. At the surface of these parts, the maximum shear stress exceeds 10 MPa. Because the inferred driving stresses (stress drops) in earthquakes are commonly only several MPa, it follows that the driving shear stress in these marginal parts is large enough to initiate or reactivate seismogenic faults. These model results are in broad agreement with data on the current seismotectonics of Fennoscandia. The formation and reactivation of tensile and shear fractures in Fennoscandia as a result of postglacial uplift is likely to increase the hydraulic conductivity of the solid rocks that constitute the uppermost part of the crust. This conclusion is supported by reported observations which indicate that the production of groundwater in wells in many areas in Norway varies positively with the maximum postglacial uplift.

Keywords: postglacial uplift; stress fields; faulting; hydrogeology; Fennoscandia

1. Introduction

Uplift and doming of the crust is currently occurring in many places at the surface of the earth. For example, doming of large volcanic fields, which may be attributed to accumulation and pressure of magma at the bottom of the crustal plate hosting the field, is common prior to the formation of collapse calderas (Gudmundsson et al., 1997). Postglacial regional doming of the crust, as a consequence of glacial unloading, has occurred in many areas, such as North America (e.g. Walcott, 1970; Koteff and Larsen, 1989; Anderson et al., 1989; Hasegawa and Basham, 1989; Wu and Hasegawa, 1996a,b), parts of Scotland (Davenport et al., 1989) and in Iceland (Ingolfsson et al., 1995).

One of the most remarkable, and certainly the best studied, large-scale crustal doming, is the postglacial

* Fax: +47 5558-4916; E-mail: agust.gudmundsson@geol.uib.no

0040-1951/99/$ – see front matter
PII: S0040-1951(99)00107-9

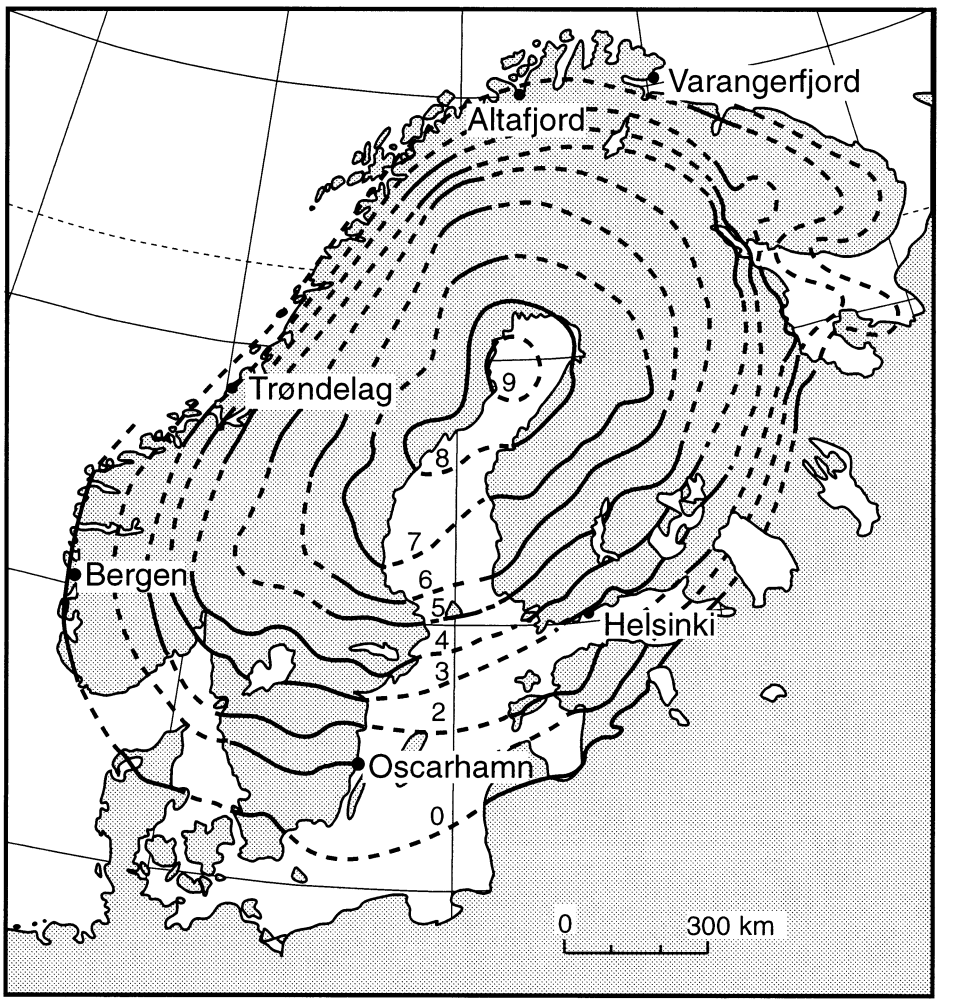

Fig. 1. Contours of the current rate of postglacial crustal uplift (doming) in Fennoscandia, in millimetres per year. The solid lines represent those areas that are covered by direct observations. Modified from Ekman (1989) and Fjeldskaar (1997). Compare with the estimated total postglacial uplift in Figs. 5 and 7.

uplift of Fennoscandia. Not only is the current rate of postglacial uplift in this region (Fig. 1) known with high accuracy (Mäkinen et al., 1986; Ekman, 1989; Scherneck et al., 1998), but the inferred total cumulative postglacial uplift is also known in great detail (Mörner, 1980). The present maximum uplift is around 760 m, but the estimated total postglacial uplift has a maximum of 850–900 m (Mörner, 1980; Stephansson, 1989).

Uplift and doming of this kind change the regional stress field and influence the tectonics of the area that is undergoing doming. Provided the uplift-related stresses are large enough, they may largely control fracture initiation and reactivation and associated seismicity in the area. For example, it is commonly suggested that a spatial correlation exists between current seismicity and postglacial uplift in some areas (Wahlström, 1989; Hasegawa and Basham, 1989; Arvidsson and Kulhanek, 1994; Klemann and Wolf, 1998), while large-scale postglacial faults have been related to stress changes due to deglaciation in other areas (Muir Wood, 1989; Arvidsson, 1996). By contrast, large ice sheets, such as in Antarctica and Greenland, may inhibit earth-

quakes, thereby explaining why the interiors of these continental areas are essentially aseismic (Johnston, 1987).

One important effect that crustal doming can have, particularly in old continental areas of otherwise little current tectonic activity, is that it may increase the hydraulic conductivity of solid rocks through the formation or reactivation of fracture systems. For example, there is an empirical correlation between production of groundwater wells in solid rocks (bedrock) in many areas of Norway and the inferred maximum postglacial uplift of these same areas (Rohr-Torp, 1994; Morland, 1997). This indicates that the stress field generated by the uplift is at least partly responsible for the current hydraulic conductivity and water production of the uppermost part of the crust.

This paper has three principal aims. First, to provide a simple mechanical model of doming with the view of improving our understanding of the associated near-surface stress field. This is done by exploring the consequences of the bending of a circular, elastic crustal plate. Second, to see if the doming-generated stresses are so large as to be able to initiate, or reactivate, fracture systems in the plate. Solutions are provided for some general cases as to the depth of propagation of tension fractures and the driving stresses of normal faults and strike-slip faults. Third, to use these general results to improve our understanding of the current seismicity and hydraulic conductivity of the upper part of the crust in Fennoscandia in general and in Norway in particular.

2. Mechanics of crustal doming

Modelling crustal doming, particularly that which results from deglaciation, has been made by many authors. A summary of earlier models, including his own, is given by Nadai (1963). More recent models include that of Walcott (1970), Stein et al. (1989), Wu and Hasegawa (1996a,b), Johnston et al. (1998), and Klemann and Wolf (1998). Commonly, crustal doming can be attributed to more than one process. For example, Rohrmann and van der Beek (1996) have suggested a Cenozoic domal uplift of southern Norway and explained this uplift in terms of an asthenospheric diapirism model. In an area subject to doming, factors such as ridge push or plate pull may also contribute to the current stress field in that area. Many authors have suggested ridge push as a major factor contributing to the current stress field in Fennoscandia, particularly in coastal areas of western Norway (e.g., Stein et al., 1989; Hicks, 1996).

The approach used in the present paper is to provide a heuristic model where the measured or estimated postglacial crustal uplift is a major factor contributing to the current stress field in Fennoscandia. Using this simple model, and the appropriate boundary conditions and elastic properties of the crust, one can calculate the near-surface stress field generated by the uplift and doming. This approach, therefore, makes it possible to infer whether or not the resulting stresses are sufficiently large so as to reactivate some of the many fracture systems that exist in Fennoscandia (e.g., Gabrielsen and Ramberg, 1979).

Many areas of crustal doming are roughly elliptical or circular in shape (Fig. 1). Here the analysis of doming is for a circular region, but it can easily be extended to an elliptic region. For a circular crustal plate subject to uniform vertical loading p at its base, the vertical displacement (doming) w of the plate is obtained from the following general governing equation for the deflection of thin, elastic plates (Ugural, 1981; Boresi and Sidebottom, 1985):

$$\nabla^4 w = \frac{p}{D} \tag{1}$$

where $\nabla^4 = \nabla^2\nabla^2 = (\nabla^2)^2$, with ∇^2 being the Laplace operator and D the flexural rigidity (resistance to deformation) of the crustal plate, given by:

$$D = \frac{Ed^3}{12(1-\nu^2)} \tag{2}$$

where E is Young's modulus, d is effective elastic thickness (Fig. 2), and ν is Poisson's ratio of the crustal plate. For the bending of a circular plate it is appropriate to use polar coordinates (Fig. 3) and assume the plate to be loaded and supported symmetrically, so that the boundary conditions are independent of the angle θ. For an axisymmetric case, where the uplift w depends only upon the radial

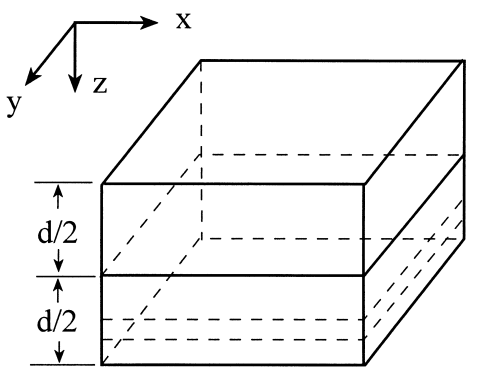

Fig. 2. Part of a circular plate subject to bending. Half thickness of the plate is $d/2$, and the axes of the coordinate system (x, y, z) are as indicated.

position r, Eq. 1 becomes the ordinary differential equation:

$$\nabla^4 w = \left(\frac{\mathrm{d}^2}{\mathrm{d}r^2} + \frac{1d}{r\,\mathrm{d}r}\right)\left(\frac{\mathrm{d}^2 w}{\mathrm{d}r^2} + \frac{1d w}{r\,\mathrm{d}r}\right) = \frac{p}{D} \qquad (3)$$

For doming of a crustal plate, there is normally no displacement of the edge of the plate. It follows that the appropriate model is that of the deflection of an elastic plate with clamped edge, in which case the boundary conditions are $w = \mathrm{d}w/\mathrm{d}r = 0$ at $r = a$. Then the vertical displacement of the plate is given by:

$$w = \frac{p}{64D}(a^2 - r^2)^2 \qquad (4)$$

The maximum uplift of the plate, $w_{\max}$, occurs at its centre, where $r = 0$, and, from Eq. 4, is:

$$w_{\max} = \frac{pa^4}{64D} \qquad (5)$$

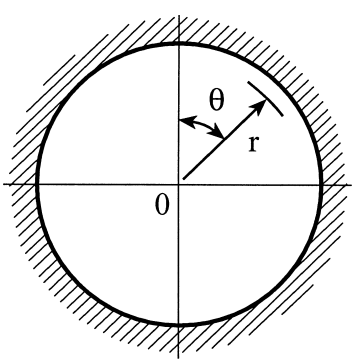

Fig. 3. For axisymmetric bending of a circular plate the polar coordinates (r, θ) are used, as is indicated here.

For axisymmetric deflection of a circular plate, the radial σ_r and circumferential σ_θ stresses are given by:

$$\sigma_r = \frac{Ez}{1-\nu^2}\left(\frac{\mathrm{d}^2 w}{\mathrm{d}r^2} + \frac{\nu\,\mathrm{d}w}{r\,\mathrm{d}r}\right) \qquad (6)$$

$$\sigma_\theta = \frac{Ez}{1-\nu^2}\left(\frac{1\mathrm{d}w}{r\,\mathrm{d}r} + \nu\frac{\mathrm{d}^2 w}{\mathrm{d}r^2}\right) \qquad (7)$$

where z is the vertical coordinate (positive upwards). Using Eqs. 4, 6 and 7, the stresses in the case of a uniformly loaded circular crustal plate, where compressive stresses are considered positive and tensile stresses negative, become:

$$\sigma_r = -\frac{3pz}{4d^3}\left[(1+\nu)a^2 - (3+\nu)r^2\right] \qquad (8)$$

$$\sigma_\theta = -\frac{3pz}{4d^3}\left[(1+\nu)a^2 - (1+3\nu)r^2\right] \qquad (9)$$

At the surface of the crustal plate, the maximum tensile stresses occur at the centre of the plate where $r = 0$ and $z = 0.5d$ (Figs. 2 and 3), and from Eqs. 8 and 9 we obtain:

$$\sigma_{\theta,\max} = \sigma_{r,\max} = -\frac{3pa^2(1+\nu)}{8d^2} \qquad (10)$$

The maximum compressive stresses, $\sigma_{r,\theta,\mathrm{com}}$, at the surface of the crustal plate occur at its edge, where $r = a$, and, from Eqs. 8 and 9, are given by:

$$\sigma_{r,\mathrm{com}} = \frac{3pa^2}{4d^2} \qquad (11)$$

$$\sigma_{\theta,\mathrm{com}} = \frac{3p\nu a^2}{4d^2} \qquad (12)$$

Using Eqs. 8 and 9, the tensile and compressive stresses anywhere in the crustal plate can be calculated. More specifically, the extreme values of the surface stresses of the domed region can be obtained from Eqs. 10–12. When these stresses are known, their effects on the formation and reactivation of tectonic fractures can be estimated, using general criteria for the initiation of tectonic fractures.

3. Mechanics of fracture formation

When the crust is subject to doming and associated stresses, all discontinuities in the crust have

the potential of concentrating stress. This follows because the discontinuities contain either relatively soft material (e.g., fault breccia or gouge) or are empty cracks, in which case the stress trajectories, whose paths must lie in the solid material, cluster together in passing around the crack. As a consequence, the magnitude and the direction of the principal stresses in the vicinity of the discontinuity are altered. Stress concentration commonly leads to reactivation of discontinuities, but the resulting slip will not necessarily have the same sense as those slips that occurred during the earlier development of the discontinuity. For example, the shallow parts of all types of faults (normal-slip, thrust- and reverse-slip, strike-slip, and oblique-slip) may be opened (reactivated as tension fractures) during doming, provided the tensile stresses are limited to the uppermost part of the crustal plate. If significant tensile stresses reach depths of many hundred metres in the crust, however, the reactivation is likely to lead to the development of normal faults.

The depth at which a pure tension (mode I) fracture changes into a normal fault can be estimated as follows. Let σ_1 denote the maximum compressive principal stress (recall that compressive stress is considered positive), σ_3 the minimum compressive principal stress, and T_0 the in-situ tensile strength of the host rock. It follows that if $\sigma_1 < -3\sigma_3$, the two-dimensional Griffith criterion for fracture initiation in the tensile stress regime, which would apply at shallow depths in the crustal plate, is given by (Jaeger and Cook, 1979, p. 101; Engelder, 1993, p. 69):

$$\sigma_3 = -T_0 \tag{13}$$

Substituting $-T_0$ for σ_3 in the inequality for the Griffith criterion above, one obtains the inequality:

$$\sigma_1 - \sigma_3 < 4T_0 \tag{14}$$

from which it follows that the stress difference for the failure criterion in Eq. 13 to apply cannot exceed $4T_0$. The vertical stress $\sigma_v(z)$ is related to the density $\rho(z)$ of the crustal plate through the formula:

$$\sigma_v(z) = \int_0^z \rho(z) g \mathrm{d}z \tag{15}$$

where g is the acceleration of gravity. If the vertical stress is the maximum compressive principal stress, so that $\sigma_v = \sigma_1$, and if the rock is homogeneous with a density of ρ_r, then Eq. 15 reduces to the familiar relation:

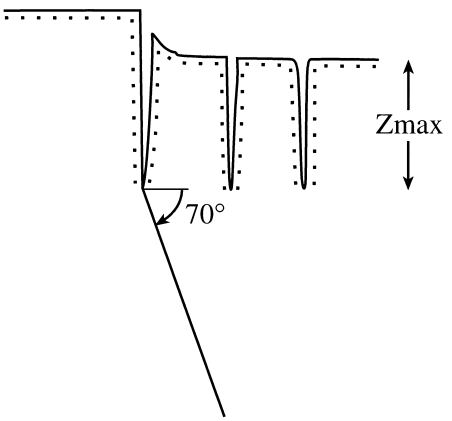

Fig. 4. Tension fracture changes into a normal fault on reaching a certain critical crustal depth z_{max} as is given by Eq. 17.

$$\sigma_1 = \rho_r g z \tag{16}$$

It follows from Eqs. 13, 14 and 16 that the maximum depth z_{max} that the tension part of a reactivated or newly formed discontinuity can reach before it changes into a normal fault is:

$$z_{max} = \frac{3T_0}{\rho_r g} \tag{17}$$

On reaching the depth indicated by this equation, a large-scale tension fracture, whether newly formed or as the topmost part of an old discontinuity, should change into a normal-fault (Fig. 4). This depth can be estimated roughly as follows. For the uppermost layer of a crustal plate, whether continental or oceanic, the in-situ rock density may be taken as roughly 2300 kg m^{-3} and the in-situ tensile strength as 1–6 MPa (Haimson and Rummel, 1982; Gudmundsson, 1983; Schultz, 1995; Amadei and Stephansson, 1997, p. 174). With $g = 9.8$ m s^{-2} and these values, Eq. 17 gives the maximum depth as $z_{max} \cong 130$–800 m. These results indicate that during doming of crustal plates, surface fractures can propagate as vertical tension fractures down to crustal depths of several hundred metres. If, however, they reach greater depths, they should change into normal faults.

When tension fractures develop in a crustal plate subject to doming, the fractures themselves decrease the effective thickness of that part of the deflected plate. This follows because no bending tensile strain

can be transmitted across the fractures. The thickness of this part of the crustal plate occupied by these fractures decreases by an amount equal to the depth of the fractures. It follows from Eqs. 2 and 3, particularly because the flexural rigidity depends on the cube of the thickness of the crustal plate, that a small reduction in the effective thickness may lead to additional doming, even though the loading at the bottom of the crustal plate remains constant. Generally, however, the magnitude of this loading is not known, and in the case of doming related to glacial rebound, it is more appropriate to calculate the doming-generated stresses from the measured or inferred uplift itself.

4. Application

In order to apply the above results to the tension fracture development and faulting in Fennoscandia, one may solve the equations for the maximum stresses in terms of the measured uplift rather than assuming some unknown loading at the bottom of the deflected crustal plate. Substituting Eq. 5 for p in Eqs. 10–12, one obtains:

$$\sigma_{\theta,\max} = \sigma_{r,\max} = -\frac{3w_{\max}64D}{4a^2d^2} \tag{18}$$

for the tensile stresses at the surface in the central part of the domed crustal plate, and:

$$\sigma_{r,\mathrm{com}} = \frac{3w_{\max}64D}{4a^2d^2} \tag{19}$$

$$\sigma_{\theta,\mathrm{com}} = \frac{3w_{\max}64D\nu}{4a^2d^2} \tag{20}$$

for the compressive stresses at the clamped edge of the plate.

In order to estimate the potential stresses during the uplift of Fennoscandia, one must know the magnitude of the uplift, as well as the thickness and properties of the elastic crust that is subject to doming. For the central part of Fennoscandia, Fjeldskaar (1997) gives the flexural rigidity as $D = 10^{24}$ Nm and the thickness of the elastic crust as $d = 50$ km. The estimated maximum postglacial uplift of the central part of Fennoscandia is 850 m (Rohr-Torp, 1994), and the average radius of the crustal dome, a, is around 750 km (Fig. 5). Substituting these values in Eq. 18 one obtains the potential maximum tensile stress due to uplift of the central part as $\sigma_\theta = \sigma_r = -29$ MPa.

The variation in the stresses, from the centre of the crustal plate to its edge, are shown in Fig. 6. Except in the central part of the plate, these stresses differ in their values, and this difference increases to a maximum at the edge of the plate. Using $\sigma_\theta = \sigma_r = 0$ in Eqs. 8 and 9, one finds that σ_θ changes to compressive stress at $r = 0.827a$ and that σ_r changes to compressive stress at $r = 0.628a$. This means that the marginal parts of the uplifted crustal plate are subject to compressive stresses, the maximum values of which are, from Eq. 19, numerically equal to the maximum tensile stress, namely 29 MPa. The differential stress $\sigma_r - \sigma_\theta$ also increases with distance from the centre of the plate and reaches its maximum absolute value at the edge itself (Fig. 6), where it is given by:

$$|\Delta\sigma_{\max}| = (1-\nu)\frac{3w_{\max}64D}{4a^2d^2} \tag{21}$$

In order to see if the maximum shear stress, $\tau_{\max}$, which is half the value in Eq. 21, would be sufficient to initiate, or reactivate, faults, one must know the criterion for faulting. The modified Griffith criterion for fracture initiation (McClintock and Walsh, 1962; Jaeger and Cook, 1979) takes into account fracture closure and associated friction during fault development, such as is likely to occur in the compressive regime of the marginal parts. If fractures start to close under very low (zero) normal stress, as is indicated by some results (Paterson, 1978), then the modified Griffith criterion in the compressive regime is presented by:

$$\mu(\sigma_1 + \sigma_3) + (\sigma_1 - \sigma_3)(1-\mu)^{1/2} = 4T_0 \tag{22}$$

where μ is the coefficient of sliding friction between the walls of the fracture, and the other symbols have the same meaning as before. This equation represents a linear relationship between the principal stresses at failure of the rock and can be rewritten as (Brace, 1960):

$$\tau = 2T_0 + \mu\sigma_{\mathrm{n}} \tag{23}$$

where σ_{n} is the normal stress on the fracture plane, and the other symbols are as defined above. Eq. 23 may be regarded as the physical basis of the well-known empirical Coulomb criterion of rock failure

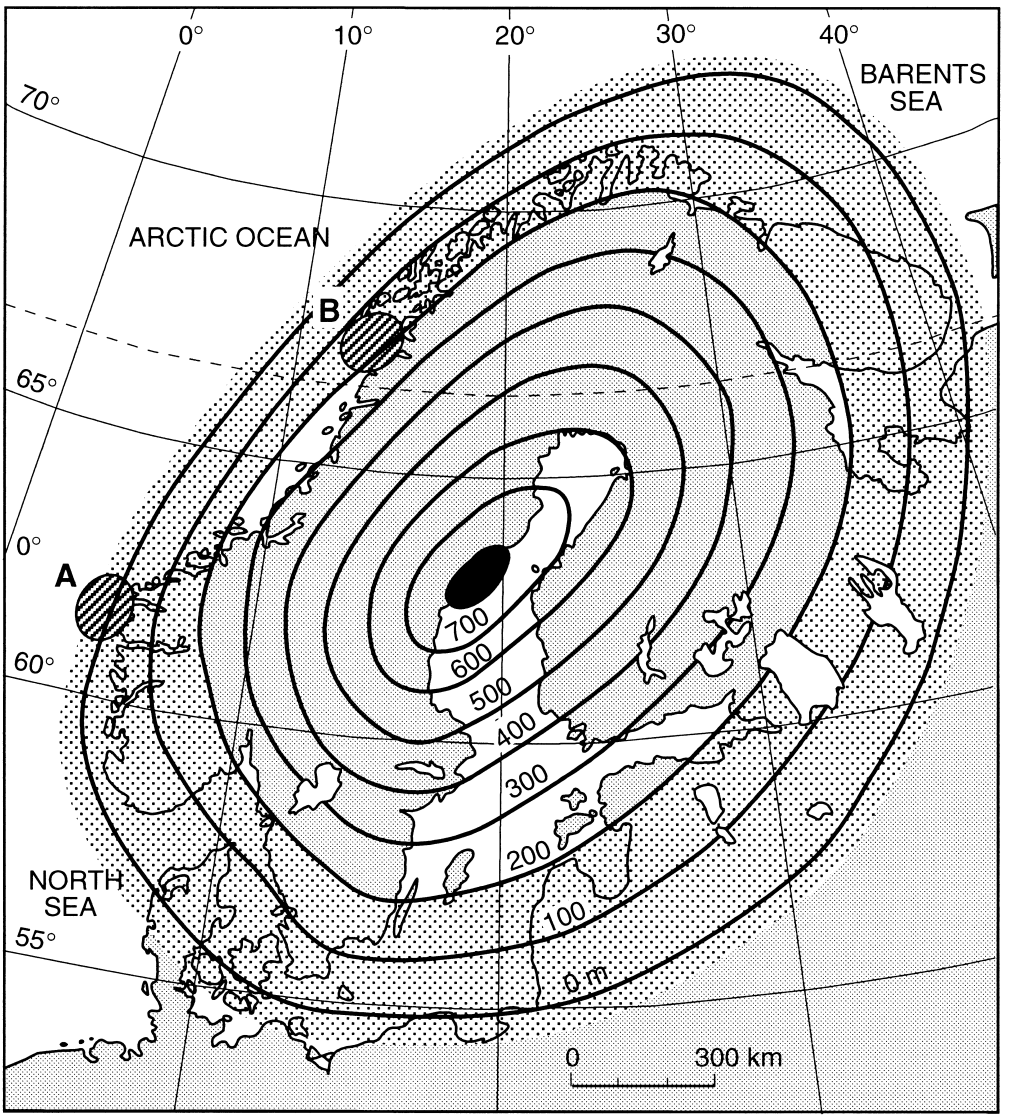

Fig. 5. Estimated total postglacial uplift in Fennoscandia (Mörner, 1980) in relation to areas of (*A*) recent strike-slip (Bungum et al., 1991) and (*B*) oblique-slip (Atakan et al., 1994) earthquakes off the western coast of Norway. According to the model presented in this paper, both these areas are largely controlled by marginal stress fields, where strike-slip and reverse faulting are to be expected. Here the shaded marginal area corresponds roughly to that part of the postglacial crustal dome where the radial stress (σ_r), as represented in Eq. 8 and in Fig. 6, is compressive.

(Brace, 1960; Jaeger and Cook, 1979). Although the last term in Eq. 23 may be very small, for most seismogenic faults, there is, nevertheless, some frictional strength $\tau_f = \mu\sigma_n$ on the fault surface subsequent to the fault slip. It follows that the driving shear stress $\Delta\tau$ is usually less than the regional shear stress, and that it can be defined as the difference between the remote (from the fault) shear stress and the residual (frictional) strength on the fault, namely as:

$$\Delta\tau = \tau - \tau_f \tag{24}$$

The driving shear stress is also commonly referred to as the (nominal) stress drop in earthquake mechanics because it is a measure of the relaxation

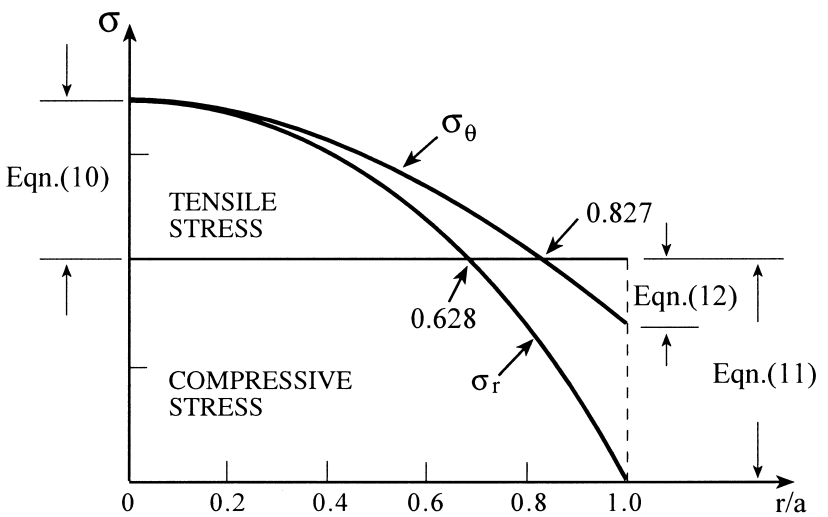

Fig. 6. Variation in radial (σ_r) and circumferential (σ_θ) stress with distance from the centre of an uplifted crustal plate. This variation in stresses is for the upper surface of the domed plate and is obtained from Eqs. 8 and 9, using a Poisson ratio of 0.3 which is appropriate for many near-surface rocks. The stresses are identical in the central part of the plate, but their difference increases with distance from the centre and the differential stress reaches a maximum at the edge of the plate. The outermost part of the crustal plate during doming is subject to high compressive stresses and also high shear stresses that encourage slip on faults.

(drop) in shear stress on a fault plane as a result of slip during an earthquake. The earthquake stress drop, however, is normally not equal to the tectonic driving shear stress. This follows because the stress drop inferred from earthquakes is related to the seismic efficiency which depends on the total or absolute stresses associated with the seismogenic fault, and these cannot be determined from seismological observations alone (cf. Scholz, 1990, p. 165; Engelder, 1993, p. 331).

All strike-slip faults, and many normal faults, can be modelled as anti-plane shear cracks (mode III cracks). Using the relation $E = 2G(1 + \nu)$, where E is Young's modulus, G is shear modulus, and ν is Poisson's ratio, the maximum relative (total) slip Δu_{max} on the fault surface (as measured in the field) is related to the driving shear stress through the equation:

$$\Delta u_{max} = \frac{4\Delta\tau(1-\nu)W}{E} \tag{25}$$

where W is the width (controlling vertical dimension) in the case of a strike-slip fault, but half the surface length in the case of a normal fault. The use of Eq. 25 for a normal fault presupposes that the total surface rupture length is the controlling (minimum) dimension and thus less than the depth (vertical dimension) of the fault (Gudmundsson, 1992, 1996). In case the surface length was greater than the depth of a normal fault, an in-plane shear crack (mode II crack) model should be used.

The numerical values obtained from Eq. 21, as well as those inferred from Fig. 6, indicate that the shear stresses near the margins of the uplifted region may exceed 10 MPa. There is much evidence that seismogenic faulting is commonly associated with zones of fluid overpressure (Gudmundsson, 1999; Gudmundsson and Homberg, 1999). When a fault plane is subject to so high fluid pressure during slip that the effective normal stress on the plane becomes zero or negative, then the term $\mu\sigma_n$ in Eq. 23 becomes essentially zero and the driving shear stress associated with faulting equal to twice the in-situ tensile strength of the rock. For tensile strengths of 1–6 MPa, the tectonic driving stress would be 2–12 MPa. Despite the potential difference between tectonic stress drop and earthquake stress drop, indicated above, these results compare well with earthquake stress drops in most large, shallow, interplate earthquakes which are between 1 MPa and 10 MPa (Kanamori and Anderson, 1975). Using these results, and the definition of driving shear

stress in Eq. 24, it follows that the shear stresses occurring near the margins of the postglacial dome in Fennoscandia are sufficient to generate slip on some of the many existing faults and fractures in those areas (Ramberg et al., 1977; Gabrielsen and Ramberg, 1979) and, presumably, also to initiate new earthquake fractures, particularly at shallow crustal levels.

5. Discussion

The results presented in this paper indicate that the stresses generated by postglacial uplift and doming of Fennoscandia are sufficiently large to initiate or reactivate fractures in this region. These results are supported by the spatial correlation between current seismicity and postglacial uplift in parts of Fennoscandia (Wahlström, 1989; Arvidsson and Kulhanek, 1994). In terms of the model proposed here, tension fractures and normal faults should dominate in the central part of the postglacial dome, whereas reverse and strike-slip faults should be more common in the marginal parts of the dome.

This conclusion seems to be in broad agreement with focal mechanisms from Fennoscandia (Arvidsson and Kulhanek, 1994; Hicks, 1996). While all types of focal mechanisms occur in the seismically active parts of Fennoscandia, there is a tendency for normal faulting to be more common in the interior parts of the uplifted crustal plate and strike-slip and reverse faulting to be more common in the marginal parts (Arvidsson and Kulhanek, 1994). In a study of the focal mechanisms of 200 earthquakes of local magnitudes 0.1–4.9, Slunga (1989) finds that strike-slip is the dominating mechanism and that most of these earthquakes occur in northern and southern Sweden. Bungum et al. (1991) studied 51 focal mechanisms in and around Norway and found that normal faulting was more common in the continental part, whereas reverse faulting (and occasionally strike-slip faulting) was more common near the coast and on the continental shelf. Bungum et al. (1991) found that strike-slip faulting was particularly common in the area just off the western coast between Sognefjorden and Nordfjorden (Fig. 5). Also, Atakan et al. (1994) analysed the January 1992 earthquake swarm in the coastal area of Steigen in northern Norway and concluded that it was associated with an oblique-slip fault.

Consideration of the seismicity of Fennoscandia over decades shows that most of the largest earthquakes occur, roughly speaking, in the marginal areas of the postglacially uplifted crustal plate. For example, a seismicity map of Fennoscandia covering the period 1951–1980 (Ringdal et al., 1982; Kinck et al., 1993) shows that nearly all earthquakes exceeding $M4$ occur in these regions (Fig. 7). These are also the regions where the crystalline crust is thinnest and where, according to the dome-model presented in this paper, one would expect shear stress to concentrate. The surface stresses generated by the uplift (Fig. 6) decrease in magnitude with depth in the crust, towards the neutral surface of the plate which, for an elastic crust of 50 km (Fjeldskaar, 1997), is at a depth of approximately 25 km. This means that postglacial doming contributes little to seismogenic faulting at about 25 km; some earthquakes are generated at this depth (Arvidsson and Kulhanek, 1994) possibly as a result of ridge push. At greater depths, postglacial doming would contribute compressive stresses to the regional stress field and thus encourage reverse or strike-slip faulting. Although there are some earthquakes down to 40 km depth in Fennoscandia (Arvidsson and Kulhanek, 1994), most earthquakes in this area are at depths less than 25 km (Bungum et al., 1991; Kinck et al., 1993), and are thus shallower than the neutral surface of the postglacial crustal doming.

In a study of the focal mechanisms of eighteen relatively large earthquakes in Sweden, Arvidsson and Kulhanek (1994) concluded that the area close to the centre of the maximum postglacial uplift has a significant extensional component. In this area, referred to as the eastern Sweden–Gulf of Bothnia zone, the focal mechanisms range from strike-slip to normal faulting and are clearly related to crustal extension. Furthermore, Arvidsson and Kulhanek (1994) find that the direction of the inferred axis of relative tension (extension) generally coincides with that of the gradient of the postglacial uplift. This means that the axis of extension is normally roughly perpendicular to the contours of the current rate of postglacial uplift (doming) in Fennoscandia (Fig. 1) and, by implications, to the contours of the total postglacial uplift (Fig. 5). These results, although based on a rather

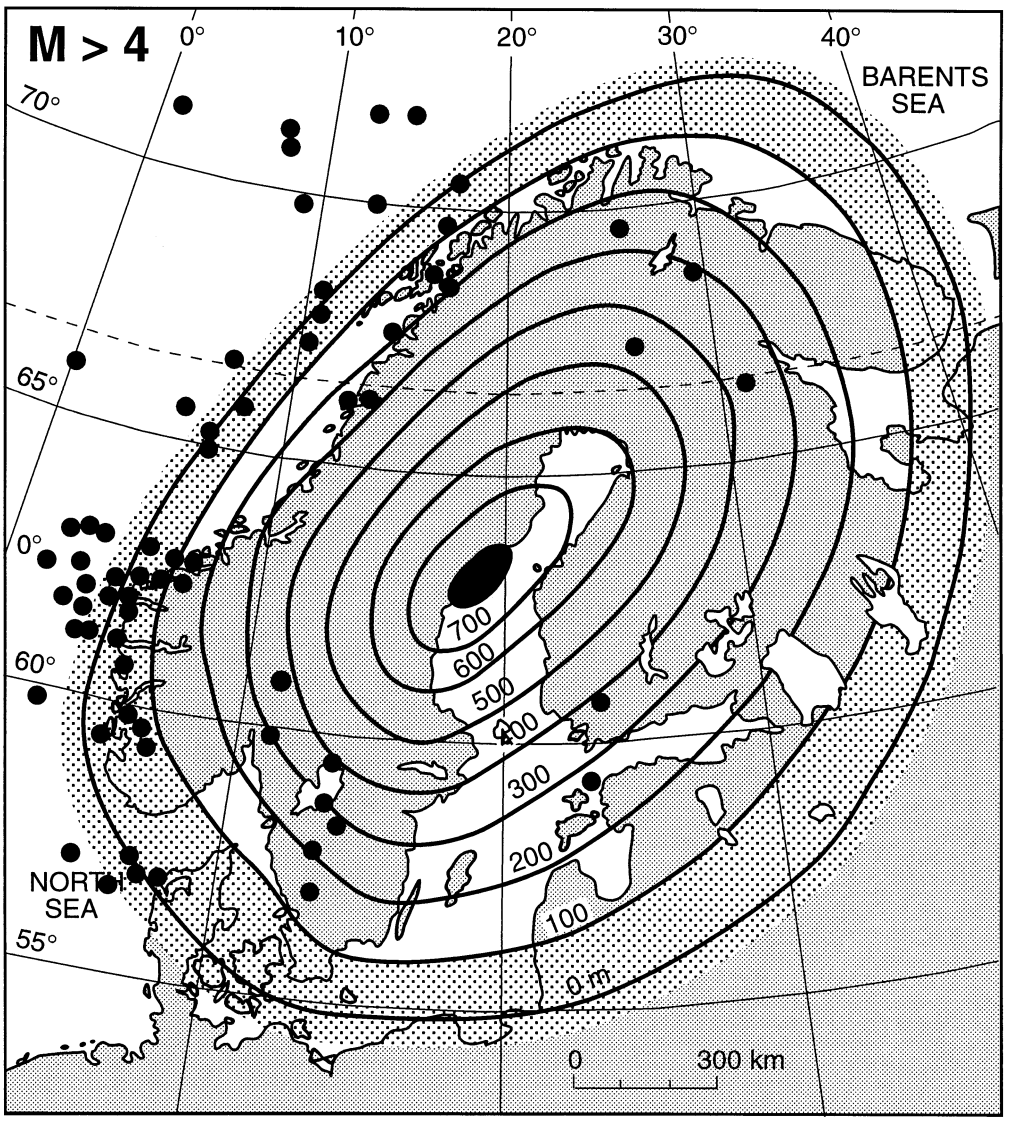

Fig. 7. Comparison of the location of 'large' ($M > 4$) earthquakes in Fennoscandia, during the period 1951–1980, and the postglacial uplift (Mörner, 1980). Data on the earthquakes from Ringdal et al. (1982) and Kinck et al. (1993). Most of these earthquakes are located inside the marginal areas of the present dome-model, where the stress fields favour reverse or strike-slip faulting. In contrast to Fig. 5, here the shaded marginal area corresponds roughly to that part of the postglacial crustal dome where both the radial (σ_r) and the circumferential (σ_θ) stresses are compressive and where the associated shear stress reaches its maximum.

limited dataset, clearly support the stress-implications of the model presented in this paper.

The model presented here has important implications for the hydraulic conductivity of the uppermost part of the crust in Fennoscandia in general and in Norway in particular. One might expect reactivation or formation of tension fractures at shallow crustal levels, normal faults at deeper levels, in the interior part of the crustal plate, but strike-slip or reverse faulting in its marginal parts, as a consequence of the postglacial uplift. As is indicated above, this type of faulting is generally confirmed by the focal mechanisms of current earthquakes. The main results from the point of view of hydrogeology would be a sig-

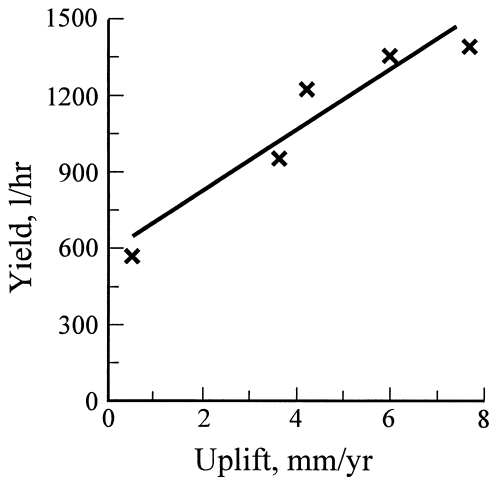

Fig. 8. Schematic presentation of the relationship between mean yield of groundwater in wells and the present rate of uplift of the areas within which these wells are located. The linear correlation coefficient $r = 0.95$. Data from Rohr-Torp (1994). The greater the current rate of uplift, and by implication the greater the total postglacial uplift, the greater is the yield of water from the wells.

nificantly increased hydraulic conductivity, and thus water production of associated wells, in the areas of greatest uplift, but less marked, and with a more complex pattern, in the marginal areas.

These predictions of the model are in broad agreement with results on the water production of wells in Norway. In a study of five areas in Precambrian rocks in southern Norway, containing a total of 1278 drilled wells, Rohr-Torp (1994) found a linear relationship between the water yield in the wells and the present uplift rates of these areas (Fig. 8). Very similar results, but based on more extensive datasets, were obtained by Morland (1997). Making the reasonable assumption that the present rate of uplift in an area is a measure of the total postglacial uplift of that area, these results indicate that the total postglacial uplift makes a major contribution to the water yield of these wells. In terms of the present model, the greater the postglacial uplift of an area, the larger will be the potential tensile stresses that can contribute to fracture formation and current hydraulic conductivity of the area. Thus, other things being equal, the total postglacial uplift should be a direct measure of the potential groundwater production of the solid rocks in Fennoscandia.

Acknowledgements

This work was supported by a grant from the Research Council of Norway and by a grant from the European Commission (contract ENV4-CT96-0252). I thank Alvar Braathen and Roy H. Gabrielsen for information on the tectonics and hydrogeology of Norway, and Hilmar Bungum, Conrad D. Lindholm, Eystein S. Husebye, Kuvvet Atakan and Erik C. Hicks for information on the earthquakes, stresses and crustal structure of Fennoscandia. I thank Roy H. Gabrielsen and the *Tectonophysics* reviewers for helpful comments on the manuscript.

References

Amadei, B., Stephansson, O., 1997. Rock Stress and its Measurement. Chapman and Hall, London, 490 pp.

Anderson, W.A., Kelley, J.T., Borns, H.W., Belknap, D.F., 1989. Neotectonic activity in coastal Maine: United States of America. In: Gregersen, S., Basham, P.W. (Eds.), Earthquakes at North-Atlantic Passive Margins: Neotectonics and Postglacial Rebound. Kluwer, Dordrecht, pp. 195–212.

Arvidsson, R., 1996. Fennoscandian earthquakes: whole crustal rupturing related to postglacial rebound. Science 274, 744–746.

Arvidsson, R., Kulhanek, O., 1994. Seismodynamics of Sweden deduced from earthquake focal mechanisms. Geophys. J. Int. 116, 377–392.

Atakan, K., Lindholm, C.D., Havskov, J., 1994. Earthquake swarm in Steigen, northern Norway: an unusual example of intraplate seismicity. Terra Nova 6, 180–194.

Boresi, A.P., Sidebottom, O.M., 1985. Advanced Mechanics of Materials. Wiley, New York, 4th ed., 763 pp.

Brace, W.F., 1960. An extension of the Griffith theory of fractures to rocks. J. Geophys. Res. 65, 3477–3480.

Bungum, H., Alsaker, A., Kvamme, L.B., Hansen, R.A., 1991. Seismicity and seismotectonics of Norway and nearby continental shelf areas. J. Geophys. Res. 96, 2249–2265.

Davenport, C.A., Ringrose, P.S., Becker, A., Hancock, P., Fenton, C., 1989. Geological investigations of late and post glacial earthquake activity in Scotland. In: Gregersen, S., Basham, P.W. (Eds.), Earthquakes at North-Atlantic Passive Margins: Neotectonics and Postglacial Rebound. Kluwer, Dordrecht, pp. 175–194.

Ekman, M., 1989. Impacts of geodynamic phenomena on systems for height and gravity. Bull. Geod. 63, 281–296.

Engelder, T., 1993. Stress Regimes in the Lithosphere. Princeton University Press, Princeton, 457 pp.

Fjeldskaar, W., 1997. Flexural rigidity of Fennoscandia inferred from the postglacial uplift. Tectonics 16, 596–608.

Gabrielsen, R.H., Ramberg, I.B., 1979. Fracture patterns in Nor-

way from Landsat imagery: results and potential use. Proc. Norwegian Sea Symposium, Tromsö, pp. 1–28

Gudmundsson, A., 1983. Stress estimates from the length/width ratios of fractures. J. Struct. Geol. 5, 623–626.

Gudmundsson, A., 1992. Formation and growth of normal faults at the divergent plate boundary in Iceland. Terra Nova 4, 464–471.

Gudmundsson, A., 1996. Geometry, displacements and driving stresses of seismogenic faults in Iceland. In: Thorkelsson, B. (Ed.), Seimology in Europe. Icelandic Meteorological Office, Reykjavik, pp. 193–198.

Gudmundsson, A., 1999. Fluid overpressure and stress drop in fault zones. Geophys. Res. Lett. 26, 115–118.

Gudmundsson, A., Homberg, C., 1999. Evolution of stress fields and faulting in seismic zones. Pure Appl. Geophys. 154 (in press).

Gudmundsson, A., Marti, J., Turon, E., 1997. Stress fields generating ring faults in volcanoes. Geophys. Res. Lett. 24, 1559–1562.

Haimson, B.C., Rummel, F., 1982. Hydrofracturing stress measurements in the Iceland research drilling project drill hole at Reydarfjordur, Iceland. J. Geophys. Res. 87, 6631–6649.

Hasegawa, H.S., Basham, P.W., 1989. Spatial correlation between seismicity and postglacial rebound in eastern Canada. In: Gregersen, S., Basham, P.W. (Eds.), Earthquakes at North-Atlantic Passive Margins: Neotectonics and Postglacial Rebound. Kluwer, Dordrecht, pp. 483–500.

Hicks, E.C., 1996. Crustal Stresses in Norway and Surrounding Areas as Derived from Earthquake Focal Mechanism Solutions and In-Situ Stress Measurements. Cand. Sci. Thesis, University of Oslo, Oslo, 164 pp.

Ingolfsson, O., Norddahl, H., Haflidason, H., 1995. Rapid isostatic rebound in southwestern Iceland at the end of the last glaciation. Boreas 24, 245–259.

Jaeger, J.C., Cook, N.G.W., 1979. Fundamentals of Rock Mechanics. Methuen, London, 3rd ed., 593 pp.

Johnston, A.C., 1987. Suppression of earthquakes by large continental ice sheets. Nature 330, 467–469.

Johnston, P., Wu, P., Lambeck, K., 1998. Dependence of horizontal stress magnitude on load dimension in glacial rebound models. Geophys. J. Int. 132, 41–60.

Kanamori, H., Anderson, D.L., 1975. Theoretical basis of some empirical relations in seismology. Bull. Seismol. Soc. Am. 65, 1073–1095.

Kinck, J.J., Husebye, E.S., Larsson, F.R., 1993. The Moho depth distribution in Fennoscandia and the regional tectonic evolution from Archean to Permian times. Precambrian Res. 64, 23–51.

Klemann, V., Wolf, D., 1998. Modelling of stresses in the Fennoscandian lithosphere induced by Pleistocene glaciations. Tectonophysics 294, 291–303.

Koteff, C., Larsen, F.D., 1989. Postglacial uplift in western New England: geologic evidence for delayed rebound. In: Gregersen, S., Basham, P.W. (Eds.), Earthquakes at North-Atlantic Passive Margins: Neotectonics and Postglacial Rebound. Kluwer, Dordrecht, pp. 105–123.

Mäkinen, J., Ekman, M., Midtsundstad, A., Remmer, O., 1986. The Fennoscandian land uplift gravity lines 1966–1984. Rep. Finnish Geod. Inst. 85, 4.

McClintock, F.A., Walsh, J.B., 1962. Friction on Griffith cracks in rocks under pressure. In: Proceedings of the Fourth U.S. National Congress on Applied Mechanics. Am. Soc. Mech. Engng., New York, Vol. 2, pp. 1015–1021.

Morland, G., 1997. Petrology, Lithology, Bedrock Structures, Glaciation and Sea Level. Important Factors for Groundwater Yield and Composition of Norwegian Bedrock Boreholes? Ph.D. Thesis, Montanuniversitat Leoben, 274 pp.

Mörner, N.A., 1980. The Fennoscandian uplift: geological data and their geodynamic implications. In: Mörner, N.A. (Ed.), Earth Rheology, Isostacy and Eustacy. Wiley, New York, pp. 251–284.

Muir Wood, R., 1989. Extraordinary deglaciation reverse faulting in northern Fennoscandia. In: Gregersen, S., Basham, P.W. (Eds.), Earthquakes at North-Atlantic Passive Margins: Neotectonics and Postglacial Rebound. Kluwer, Dordrecht, pp. 141–173.

Nadai, A., 1963. Theory of Flow and Fracture of Solids. McGraw-Hill, New York, Vol. 2, 705 pp.

Paterson, M.S., 1978. Experimental Rock Deformation — The Brittle Field. Springer, Berlin, 254 pp.

Ramberg, I.B., Gabrielsen, R.H., Larsen, B.T., Sollit, A., 1977. Analysis of fracture pattern in southern Norway. Geol. Mijnbouw 56, 295–310.

Ringdal, F., Husebye, E.S., Bungum, H., Mykkelveit, S., Sandvin, O.A., 1982. Earthquake hazard offshore Norway: a study for the NTNF safety offshore program. NTNF/NORSAR, Kjeller, Oslo, 64 pp.

Rohrmann, M., van der Beek, P., 1996. Cenozoic postrift domal uplift of North Atlantic margins: an astenospheric diapirism model. Geology 24, 901–904.

Rohr-Torp, E., 1994. Present uplift rates and groundwater potential in Norwegian hard rocks. Bull. Nor. Geol. Unders. 426, 47–52.

Scherneck, H.G., Johansson, J.M., Mitrovica, J.X., Davis, J.L., 1998. The BIFROST project: GPS determined 3-D displacement rates in Fennoscandia from 800 days of continuous observations in the SWEPOS network. Tectonophysics 294, 305–321.

Scholz, C.H., 1990. The Mechanics of Earthquakes and Faulting. Cambridge University Press, Cambridge, 439 pp.

Schultz, R.A., 1995. Limits of strength and deformation properties of jointed basaltic rock masses. Rock Mech. Rock Eng. 28, 1–15.

Slunga, R.S., 1989. Focal mechanisms and crustal stresses in the Baltic Shield. In: Gregersen, S., Basham, P.W. (Eds.), Earthquakes at North-Atlantic Passive Margins: Neotectonics and Postglacial Rebound. Kluwer, Dordrecht, pp. 261–276.

Stein, S., Cloetingh, S., Sleep, N.H., Wortel, R., 1989. Passive margin earthquakes, stresses and rheology. In: Gregersen, S., Basham, P.W. (Eds.), Earthquakes at North-Atlantic Passive Margins: Neotectonics and Postglacial Rebound. Kluwer, Dordrecht, pp. 231–259.

Stephansson, O., 1989. Stress: measurements and modelling of crustal rock mechanics in Fennoscandia. In: Gregersen, S.,

Basham, P.W. (Eds.), Earthquakes at North-Atlantic Passive Margins: Neotectonics and Postglacial Rebound. Kluwer, Dordrecht, pp. 213–229.

Ugural, A.C., 1981. Stresses in Plates and Shells. McGraw-Hill, New York, 317 pp.

Wahlström, R., 1989. Seismodynamics and postglacial faulting in the Baltic Shield. In. Gregersen, S., Basham, P.W. (Eds.), Earthquakes at North-Atlantic Passive Margins: Neotectonics and Postglacial Rebound. Kluwer, Dordrecht, pp. 467–482.

Walcott, R.I., 1970. Isostatic response to loading of the crust in Canada. Can. J. Earth Sci. 7, 716–727.

Wu, P., Hasegawa, H.S., 1996a. Induced stresses and fault potential in eastern Canada due to a disc load: a preliminary analysis. Geophys. J. Int. 125, 415–430.

Wu, P., Hasegawa, H.S., 1996b. Induced stresses and fault potential in eastern Canada due to a realistic load: a preliminary analysis. Geophys. J. Int. 127, 215–229.